

Efficiency of Chemically Activated Carbon Derived from Palmyra Palm Shell for Water Hardness Removal

Tinnapan Netpae

Department of Applied Science, Nakhon Sawan Rajabhat University, Nakhon Sawan, Thailand.

Received on December 21, 2024, Accepted on February 19, 2025

Abstract

The primary goal of this study was to examine the efficiency of Palmyra palm shell activated carbon (PPSAC) generated through chemical activation in eliminating hardness from synthetic water. Locally available palmyra palm shells from Nakhon Sawan province, Thailand, were used as raw materials for activated carbon production. The Palmyra palm shells were heated at 400 °C and 500 °C for varying durations of 1, 2, and 3 hours. The activation processes utilized H_3PO_4 , ZnCl_2 , and KOH as activating agents. The optimal carbonization temperature identified in the research was 500 °C with 2 hours of activation time. The highest iodine adsorption of 884 mg/g was achieved with PPSAC using 30% H_3PO_4 at a ratio of 1:3 (charcoal to H_3PO_4) at 500°C for 1 hour. The removal efficiency of CaCO_3 decreased gradually following contact time at 2 hours. SEM analysis revealed the presence of calcium ions on the PPSAC surface became evident. Equilibrium data were analyzed by Langmuir, Freundlich, and Temkin adsorption isotherm models. The graphical representation of adsorption isotherms indicated that the adsorption of CaCO_3 on PPSAC through H_3PO_4 activation followed the Freundlich adsorption model, with a highest adsorption capacity (K_F) of 10.50 mg CaCO_3 /g at equilibrium.

© 2025 Jordan Journal of Earth and Environmental Sciences. All rights reserved

Keywords: Hardness, Palmyra palm shell, Activated carbon, Adsorption, Isotherm

1. Introduction

Globally, hardness is a significant concern in water quality management. Primarily attributed to calcium ions (Ca^{2+}) and magnesium ions (Mg^{2+}), it also involves other cations like aluminum (Al^{3+}) and ferrous ions (Fe^{2+}). While hard water doesn't directly jeopardize health, it does impede the efficacy of soaps and detergents. Additionally, its mineral content, including calcium carbonate (CaCO_3), calcium sulfate (CaSO_4), and magnesium hydroxide ($\text{Mg}(\text{OH})_2$), can accumulate in pipes and boilers. This buildup reduces water flow and compromises heating efficiency. Carbonate hardness shows heightened sensitivity to high-temperature water. Calcium and magnesium salts also form hard scales in industrial boilers. Addressing water hardness is imperative for industries to avoid economic losses due to equipment failures and maintenance issues, which often result in unplanned shutdowns for repairs and cleanings. Soda ash and lime are highly effective and commonly used to reduce water hardness through chemical reactions, but they can be very expensive when treating large volumes of water (Brandt et al., 2016). In 2022, the global water hardness treatment market was valued at USD 1,728 million (Business Research Insights, 2023).

Activated carbon, known for its high absorption efficiency, is an essential material widely used for filtering harmful chemicals from water and air pollution. It's derived from graphite and processed to generate numerous small pores between carbon atoms. Researchers have explored low-cost activated carbon adsorbents from agricultural by-products, such as coconut shells, cashew nut shells, pineapple

peels, and drumstick tree seed husks to remove hardness ions from water (China, 2016; Rolence et al., 2014; Ashtaputrey and Ashtaputrey, 2016; Khati, 2018).

The Palmyra palm (*Borassus flabellifer* Linn.) is a vital palm species within the sugar palm group, widely found in tropical Asian countries, including Thailand. Its fruits contain sweet, fibrous flesh encased in a hard shell. Despite being a significant economic resource for various communities, the palm's shell is typically discarded as waste after seed extraction. This study examines the viability of utilizing activated carbon derived from Palmyra palm shells (PPSAC) via chemical activation with different agents (H_3PO_4 , ZnCl_2 , and KOH) for the adsorption of calcium hardness in water (expressed as mg CaCO_3 /L). It delves into the efficiency of PPSAC under varied conditions like contact time and initial concentration. The objective of this study is to evaluate the adsorption capacity of PPSAC and understand potential adsorption mechanisms through analyzing three distinct adsorption isotherms.

2. Materials and methods

2.1 Adsorbate preparation

Synthetic hardness water was produced by dissolving 1.19 g CaCl_2 and 1 g MgSO_4 into 1 L of deionized water. The solution's pH value was adjusted with 0.1 mol/L of HCl or NaOH until it reached pH 6.8 (Rolence et al., 2014)) and served as the synthetic hardness water stock.

2.2 Adsorbents preparation

Palmyra palm shell samples were collected from a local food processing community enterprise in Chum Saeng

* Corresponding author e-mail: tinnapan.n@nsru.ac.th

district in Nakhon Sawan province, located in the lower northern region of Thailand. Chum Saeng district has a tropical savanna climate with average temperatures that range from 26 °C to 32 °C. The region receives 1,475 mm of rainfall annually, with high humidity and heavy rain from June to October.

Initially, the Palmyra palm shells were washed and oven-drying at 50°C for 12 hours. Dried shells were carbonized into charcoal at temperature at 400 °C and 500 °C at the intervals of 1, 2, and 3 hours in the muffle furnace. After that, Palmyra palm shell charcoals were crushed in a mortar and mesh-sieved to obtain particles with a diameter of less than 150 µm. The charcoal was determined for physical properties by methods of American Society for Testing and Materials (ASTM). The percentage of moisture content, volatile matter, and ash content were assessed using ASTM 3173 (2012), ASTM D 3175 (2012), and ASTM D 3174 (2012) methods, respectively.

The percentage of fixed carbon (FC) in charcoal was calculated by subtracting the summation moisture content (Mc), ash content (Ac), and volatile matter (Vm) from 100% (equation 1).

$$FC (\%) = 100\% - Mc (\%) + Ac (\%) + Vm (\%) \quad (1)$$

Subsequently, a concentration of 30% (w/v) $ZnCl_2$, KOH, and H_3PO_4 solution was used for chemical activation with the ratio of ground charcoal to activating solutions ranging from 1:0 to 1:4 (w/v).

To ensure adequate penetration of the activating agent, the mixtures were agitated for 24 hours at room temperature ($28 \pm 2^\circ C$) and 150 rpm. Afterwards, the samples were washed with deionized water until reaching a pH of 7.0 ± 0.1 , followed by drying overnight in an oven at 50 °C. The dried material was activated for an hour at 500 °C in a muffle furnace. After that, the dried material was cooled to room temperature. All activated carbons produced were sieved to a particle less than 150 µm and collected in plastic containers for further analysis (Figure 1).

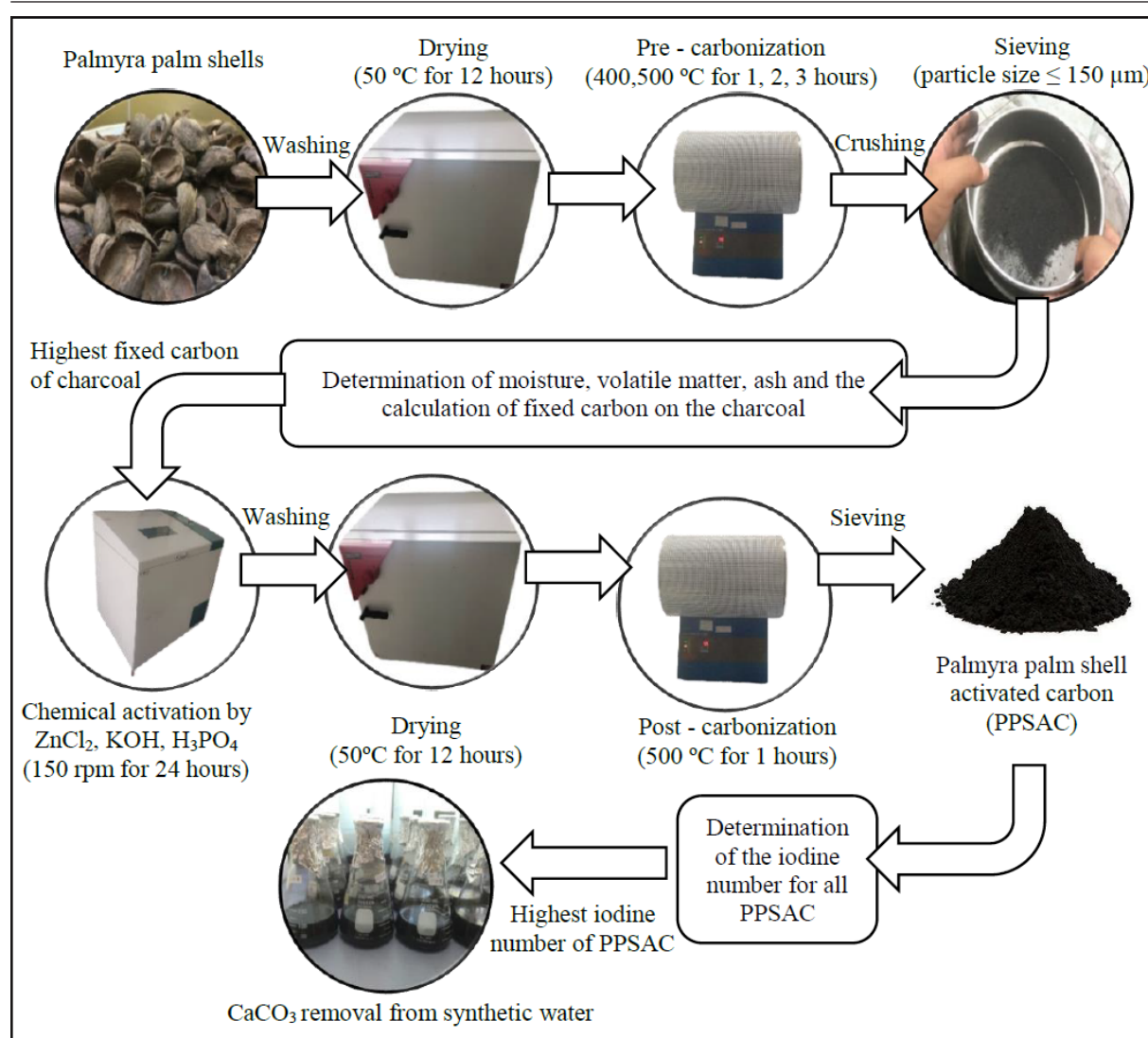


Figure 1. The schematic diagram of PPSAC powder prepared by chemical activation for $CaCO_3$ adsorption from synthetic water.

2.3 Characterization of PPSAC adsorbent

The iodine number was determined for all PPSAC adsorbents based on ASTM D 4607-86 (2006), using the sodium thiosulphate volumetric method. This served as a measure of the activated carbon's activity level or micropore content. The iodine value is a key parameter for evaluating the activity of activated carbon. A higher iodine value indicates more activation. The iodine number (mg/g) represents the amount of iodine (I_2) in milligrams adsorbed per gram of PPSAC from an iodine solution (Ashtaputrey and Ashtaputrey, 2016).

2.4 Effects of concentration and contact time on the efficiency of hardness adsorption by PPSAC

The adsorption efficiency of PPSAC was conducted by contacting 1 g of the PPSAC with 100 mL of synthetic water at different concentrations (100 to 500 mg/L as $CaCO_3$) on a rotary shaker at 150 rpm and room temperature ($28 \pm 2^\circ C$). The contact time on the hardness sorption was determined between 30 minutes to 4 hours. The samples were collected at various intervals and analyzed for hardness concentration using the EDTA titrimetric method (APHA, AWWA, WEF, 2017).

The amount of hardness uptake by the PPSAC is expressed as follows: equation 2.

$$q = C_i - C_f \times V \times W \quad (2)$$

In equation 2, q is the hardness uptake (mg $CaCO_3$ /g dry mass), whereas C_i and C_f are the initial and the equilibrium concentrations of $CaCO_3$ in the solution (mg/L), respectively. V is the volume of synthetic water (mL), and W is the weight of activated carbon used (g).

Scanning electron microscopy (SEM- Hitachi S-3500, Japan) was used to examine the microstructure changes of the PPSAC surface before and after hardness adsorption. The PPSAC samples were covered with a thin layer of carbon, and the electron-accelerated voltage of the microscope used for imaging was set at 20 kV.

2.5 Adsorption isotherm models

The linearization analysis has been one of the most applied tools for defining the best-fitting adsorption isotherm models due to its mathematical simplicity (Al-Shaybe and Khalili, 2009; Al-Haj-Ali and Marashdeh, 2014). The isotherm models analyzed in this experimental data were the Langmuir, Freundlich, and Temkin equations.

Equilibrium in the adsorption process is quickly established between the amount of hardness adsorbed onto the activated carbon (q_e , mg/g) and the quantity of hardness remaining in the solution (C_e , mg/L).

The Langmuir isotherm model is utilized for monolayer sorption on a homogeneous site on the surface of the sorbent. The Langmuir isotherm model is represented by the following equation 3.

$$1/q_e = (1/q_m K_L) (1/C_e) + 1/q_m \quad (3)$$

In equation 3, K_L is the Langmuir isotherm constant, while q_m is the maximum monolayer adsorption capacity, while $1/q_e$ represents the slope and $1/C_e$ serves as the intercept on the vertical axis (Langmuir, 1916).

On the other hand, the Freundlich isotherm model is commonly applied to illustrate the adsorption characteristics of heterogeneous surfaces. The equation for the Freundlich isotherm model is represented by the following equation 4:

$$\log q_e = (1/n) \log C_e + \log K_F \quad (4)$$

The Freundlich constant (K_F) and adsorption intensity ($1/n$) are obtained directly from the slope and intercept by plotting $\log q_e$ versus $\log C_e$. The value of n is generally between 2 to 10. K_F (mg/g) represents the adsorption or distribution coefficient, indicating the amount of dye adsorbed onto the adsorbent at one unit of equilibrium concentration (Freundlich, 1906).

The Temkin isotherm incorporates a factor that explicitly accounts for the interactions between the adsorbent and adsorbate. The linearized form of the Temkin isotherm model is represented by the following equation 5:

$$q_e = B_T \ln A_T + B_T \ln C_e \quad (5)$$

where A_T is the Temkin isotherm equilibrium constant (mg/L), B_T is the constant related to the heat of sorption (J/mol), R is the universal gas constant (8.314 J/mol/K), T is the absolute temperature (298K), and B_T is Temkin isotherm constant or R_T/B_T . A plot of q_e versus $\ln C_e$ makes possible the determination of the isotherm B and KT constants from the slope and the intercept, respectively (Temkin, 1940).

2.6 Statistical analysis

All laboratory experiments were done three times, and mean values were subjected to one-way ANOVA and Post Hoc Duncan's test ($p < 0.05$) for statistical analysis.

3. Results and discussions

3.1 Physical properties of Palmyra palm shell charcoal

Variations in the physical properties of charcoal were evident across different carbonization temperatures and durations. As the carbonization temperature increased from $400^\circ C$ to $500^\circ C$, the moisture and volatile matter percentages decreased, while the ash content increased, especially with prolonged carbonization periods. The highest fixed carbon (72.72%) was achieved at a carbonization temperature of $500^\circ C$ for 2 hours, indicating optimal conditions for char formation (Table 1). The significance of fixed carbon content lies in its role in adsorption, where the carbon surface retains adsorbate molecules through weak Van der Waals forces (McDougall, 1991; Sharififard, 2018). Consequently, a higher fixed carbon content corresponds to a larger carbon surface area available for adsorption of the adsorbate (Paethanom and Yoshikawa, 2012).

Values with the same superscript letters within each column are not significantly different at $p < 0.05$ based on Duncan's multiple range test.

Furthermore, the percentage of fixed carbon in charcoal derived from Palmyra palm shells at $500^\circ C$ for 2 hours (72.72%) closely rivaled that of bamboo charcoal (73.15%), coconut shell charcoal (74.35%), and conventional charcoal (77.20%) (Mahanim et al., 2011; Nukman et al., 2014; Njenga et al., 2016). Notably, it surpassed the fixed carbon content found in silky oak charcoal (56.2 ± 0.63) and mangrove charcoal (68.78%) (Njenga et al., 2016; Rahman et al., 2019).

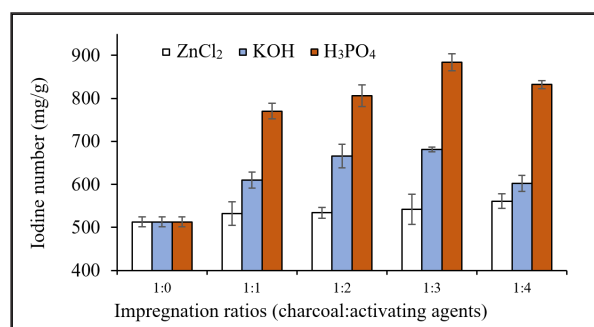
Table 1. The physical properties of palmyra palm shell charcoal were assessed at varying carbonization durations (1, 2, and 3 hours) and two different temperatures.

Carbonization temperature (°C)	Time (hours)	Moisture content (%)	Volatile matter content (%)	Ash content (%)	Fixed carbon (%)
400	1	8.99±1.06 ^d	13.46±1.93 ^e	10.96±1.08 ^a	66.59
	2	8.84±0.47 ^{cd}	12.68±2.76 ^{de}	11.88±0.83 ^{ab}	66.60
	3	8.60±1.33 ^c	11.13±1.92 ^d	12.77±0.94 ^b	67.50
500	1	7.72±1.05 ^b	7.44±1.70 ^c	14.17±1.08 ^c	70.67
	2	6.42±0.80 ^a	6.51±1.20 ^b	14.35±0.83 ^c	72.72
	3	6.40±1.01 ^a	6.35±0.81 ^a	18.61±1.03 ^d	68.64

3.2 Effect of the impregnation ratio of PPSAC with chemical agents on iodine number

Chemical activation was conducted using Palmyra palm shells, which were charred at a temperature of 500 °C for 2 hours. Figure 2 illustrates the iodine number of the activated carbon alongside the chemical agents employed for activation. The results indicate that all activated carbons exhibited superior adsorption efficiency compared to charcoal. Notably, activated carbon impregnated with H_3PO_4 demonstrated the highest iodine number, while the lowest iodine number was observed for activated carbon impregnated with $ZnCl_2$ and KOH.

Phosphoric acid acts as a catalyst, promotes bond cleavage reactions, and facilitates crosslinking through cyclization, condensation, and combines with organic species to form phosphate and polyphosphate esters. These mechanisms assist in preserving the internal pore structure and prevent excessive burning of the adsorbent during carbon activation (Xu et al., 2014).

**Figure 2.** The iodine number was investigated to assess the effect of impregnation ratio of PPSAC with chemical agents ($ZnCl_2$, KOH, and H_3PO_4).

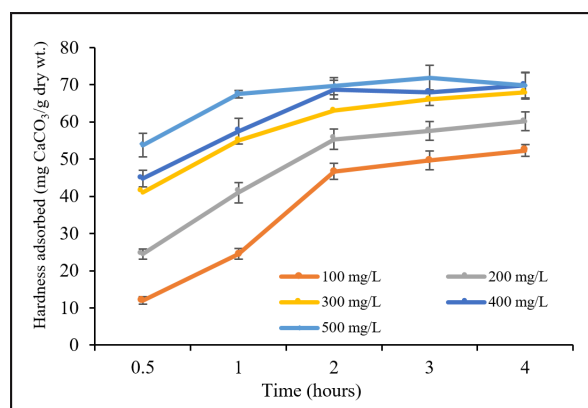
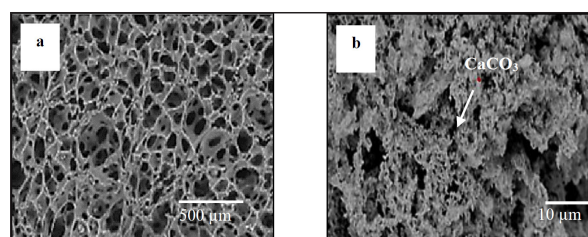
The impregnation ratio between charcoal and H_3PO_4 increased from 1:1 to 1:3, increasing the adsorbed $CaCO_3$ volume. Similarly, the iodine value of the PPSA activated with H_3PO_4 was increased from 770 to 884 mg/g as the ratio increased. The elevated iodine number observed in PPSA confirms its developed micropore structure and indicates a good adsorption capacity.

This increase may result from chemisorption within the pores during activation and leads to variations in reactivity with different activating agents and subsequent enhancement in pore structure (Sahira et al., 2013). Consequently, a charcoal to H_3PO_4 impregnation ratio of 1:3 showed the best adsorption capacity. It was selected to evaluate the effectiveness of $CaCO_3$ adsorption.

3.3 Effect of Initial Concentration and Contact Time on Hardness Removal by PPSAC with H_3PO_4 Activation

Figure 3 illustrates the impact of $CaCO_3$ concentration (100, 200, 300, 400, and 500 mg/L) and contact time (30 minutes, 1, 2, 3, and 4 hours) on the hardness adsorption by Palmyra palm shell activated carbon (PPSAC), carbonized at 500 °C and prepared with 30% H_3PO_4 at a ratio of 1:3. Initially, the adsorption of $CaCO_3$ increases with rising concentration, plateauing beyond 400 mg/L. The removal efficiency escalates rapidly up to the optimum time (2 hours) due to ample active binding sites. However, as concentration and contact time increase, hardness ion removal diminishes steadily, likely due to decreased availability of adsorption sites (Ugwu et al., 2020). Eventually, the adsorption process becomes less efficient due to surface saturation with calcium ions (China, 2016).

SEM analysis, depicted in Figure 4(a), reveals numerous micron-sized pores on the surface of PPSAC, attributed to carbonization at 500 °C and H_3PO_4 activation. Subsequently, Figure 4(b) shows SEM images of the adsorbent after $CaCO_3$ adsorption, indicating the presence of calcium ions on the PPSAC surface. The activation process not only preserved the structure but also facilitated homogeneous pore distribution (Stc, 2011).

**Figure 3.** Effect of initial concentration and contact time on hardness removal efficiency by PPSAC with H_3PO_4 activation at 1:3 ratio.**Figure 4.** SEM images of PPSAC surface before (a) and after (b) $CaCO_3$ adsorption by H_3PO_4 activation.

3.4 Adsorption isotherms study

The Freundlich isotherm better fits the adsorption of hardness onto PPSAC by H_3PO_4 activation in a 1:3 ratio compared to the Langmuir and Temkin isotherms, as indicated by correlation coefficients exceeding 0.9866 (Figure 5). The adsorption capacity or Freundlich constant (K_F) and intensity ($1/n$) of the Freundlich isotherm were determined to be 10.50 mg CaCO_3/g , and 0.3612, respectively (Table 2). The adsorption capacity of CaCO_3 by PPSAC after activation with H_3PO_4 observed in this work was higher than other activated carbons prepared by different sources, such as moringa seed pod husk (Khathi, 2018), cashew nut

shell (China, 2016), coconut shell (Rolence et al., 2014), but lower than pitombeira seeds, presenting K_F values 19.05 mg CaCO_3/g (Mendonça et al., 2022). A value of $1/n$ between 0 and 1 signifies favorable adsorption, with the Freundlich isotherm showing high adsorbent loadings at higher concentrations ($n > 1$) (Worch, 2012). This model assumes multi-layer absorption and heterogeneous surface characteristics, making it widely applicable for describing activated carbon adsorption in wastewater treatment (Budhiary and Sumantri, 2020). These findings demonstrate the potential of economically viable PPSAC for efficient water hardness removal.

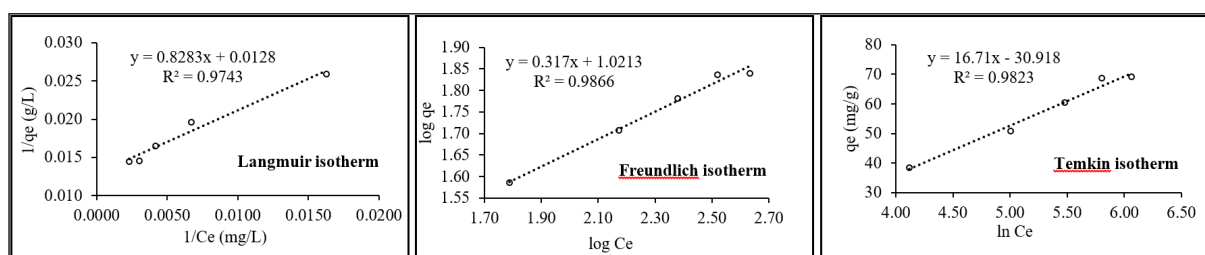


Figure 5 The isotherm curves depict the efficiency of hardness removal by PPSAC through H_3PO_4 activation at a 1:3 ratio, with a contact time of 2 hours.

Table 2. Comparison of the Langmuir, Freundlich, and Temkin constants for the adsorption of hardness onto PPSAC by H_3PO_4 activation at a 1:3 ratio.

Langmuir isotherm			Freundlich isotherm			Temkin isotherm		
q_m (mg/g)	K_L	R^2	$1/n$	K_F (mg/g)	R^2	B_T	A_T (L/mg)	R^2
82.64	0.0146	0.9743	0.3612	10.50	0.9866	16.71	0.1572	0.9823

4. Conclusions

The findings of this study demonstrate that PPSAC exhibits significant potential for removing hardness from aqueous solutions. Optimal adsorption occurred at a contact time of 2 hours. The process of hardness adsorption by PPSAC through H_3PO_4 activation at a 1:3 ratio adheres well to the Freundlich adsorption isotherm equation, with a correlation coefficient of 0.9866 and the highest adsorption capacity of 10.50 mg CaCO_3/g .

Acknowledgment

I am grateful to acknowledge the financial support provided by the Faculty of Science and Technology at Nakhon Sawan Rajabhat University, Thailand.

References

- Al-Haj-Ali, A.M., Marashdeh, L.M. (2014). Removal of Aqueous Chromium (III) Ions Using Jordanian Natural Zeolite Tuff in Batch and Fixed Bed Modes. *Jordan Journal of Earth and Environmental Sciences*, 6 (2): 45-51.
- Al-Shaybe, M. and Khalili, F. (2009). Adsorption of Thorium (IV) and Uranium (VI) by Tulul alShabba Zeolitic Tuff, Jordan. *Jordan Journal of Earth and Environmental Sciences*, 2 (Special Publication 1): 108-119.
- APHA, AWWA, WEF. (2017). Standard methods for the examination of water and wastewater. 23rd Edition, American Public Health Association, American Water Works Association, Water Environment Federation, Denver.
- Ashtaputrey, S.D., and Ashtaputrey, P.D. (2016). Preparation, characterization and application of pineapple peel activated carbon as an adsorbent for water hardness removal. *Journal of Chemical and Pharmaceutical Research*, 8: 1030-1034.
- ASTM D 3173. (2012). Standard test method for moisture in

the analysis sample of coal and coke. Annual book of ASTM standard Vol 05, Philadelphia, D3173-11.

ASTM D 3174. (2012). Standard test method for ash in the analysis sample of coal and coke. Annual book of ASTM standard. Vol 05, Philadelphia, D3174-11.

ASTM D 3175. (2012). Standard test method for volatile in the analysis sample of coal and coke. Annual book of ASTM standard. Vol 05, Philadelphia, D3175-11.

ASTM D 4607. (2006). Standard test method for determination of iodine number of activated carbon, Annual book of ASTM standard. Vol 03, Philadelphia, D 4607-86.

Brandt, M.J., Johnson, K.M., Elphinston, Andrew, Ratnayaka, D.D. (2016). *Twort's Water Supply*. 7th Ed., Butterworth-Heinemann, Oxford.

Budhiary, K.N.S., and Sumantri, I. (2020). Langmuir and Freundlich isotherm adsorption using activated charcoal from banana peel to reduce total suspended solid (TSS) levels in tofu industry liquid waste. *International Conference on Chemical and Material Engineering*, 1053, 012113.

Business Research Insights. (2023). Global water hardness removal industry research report 2023, competitive landscape, market size, regional status and prospect. *Maia-22374995*, 123.

Freundlich, H.M.F. (1906). Over the adsorption in solution. *The Journal of Physical Chemistry A*, 57: 385-471.

Khathi, V.V. (2018). Adsorption studies on water hardness removal by using Moringa oleifera seed pod husk activated carbon as an adsorbent. *International Journal of Life Sciences*, 12: 1-8.

Langmuir, I. (1916). The constitution and fundamental properties of solids and liquids, Part. I: Solids. *Journal of the American Chemical Society*, 38: 2221-2295.

Mahanim, S. MA., Ibrahim, W.A., Jalil, R., Elham, P. (2011). Production of activated carbon from industrial bamboo waste.

Journal of Tropical Forest Science, 23: 417-424.

McDougall, G.J. (1991). The physical nature and manufacture of activated carbon. *Journal- South African Institute of Mining and Metallurgy*, 91: 109-120.

Mendonca, J.C., Cantanhede, L.B., Rojas, M.O.A.I., Rangel, J.H.G., Bezerra, C.W.B. (2022). Preparation of activated charcoal adsorbent from pitombeira seeds (*Talisia esculenta*) and its application for Ca^{2+} ions removal. *Water Supply*, 22 (1): 481–495.

Njenga, M., Mahmoud, Y., Mendum, R., Iiyama, M. Jamnadass R., Roing de Nowina, K., Sundberg, C. (2016). Quality of charcoal produced using micro gasification and how the new cook stove works in rural Kenya. *Environmental Research Letters*, 12, 095001.

Nukman, Sipahutar, R., Yani, I., Arief, T. (2014). The blending effect of coalite, coconut shell charcoal and gelam wood charcoal on calorific value. *American Journal of Applied Sciences*, 11: 833-836.

Paethanom, A., and Yoshikawa, K. (2012). Influence of pyrolysis temperature on rice husk char characteristics and its tar adsorption capability. *Energies*, 5: 4941-4951.

Rahman, R., Widodo, S., Azikin, B., Tahir, D. (2019). Chemical composition and physical characteristics of coal and mangrove wood as alternative fuel. *Journal of Physics: Conference Series*, 1341: 052008.

China, C.R. (2016). Adsorption studies on water hardness removal by using cashew nut shell activated carbon as an adsorbent. *African Journal of Science and Research*, 4: 78-81.

Rolence, C., Machunda, R.L., Njau, K.N. (2014). Water hardness removal by coconut shell activated carbon. *International Journal of Science, Technology and Society*, 2: 97-102.

Sahira, J., Mandira, A., Prasad, B.P., Ram, R.P. (2013). Effect of activating agents on the activated carbons prepared from lapsi seed stone. *Research Journal of Chemical Sciences*, 3: 19-24.

Sharififard, H., Lashanizadegan, A., Pazira, R., Darvishi, P. (2018). Xylene removal from dilute solution by palm kernel activated charcoal: Kinetics and equilibrium analysis. *Advances in Environmental Technology*, 4: 107-117.

Stc, H. (2011). Characterization of activated carbons produced from oleaster stones. *InTech*.

Temkin, M.I., and Pyzhev, V. (1940). Kinetics of ammonia synthesis on promoted iron catalyst. *Acta Physicochimica*, 12: 217-222.

Ugwu, E.I., Tursunov, O., Kodirov, D., Shaker, L., Al-Amiery, A.A., Yangibaeva, I., Shavkarov, F. (2020). Adsorption mechanisms for heavy metal removal using low cost adsorbents: A review. *IOP Conference Series: Earth and Environmental Science*, 614, 012166.

Worch, E. (2012). Adsorption technology in water treatment: fundamentals, processes, and modeling, De Gruyter, Boston.

Xu, J., Chen, L., Qu, H., Jiao, Y., Xie, J., Xing, G. (2014). Preparation and characterization of activated carbon from reedy grass leaves by chemical activation with H_3PO_4 . *Applied Surface Science*, 320: 674-680.